

# Collisional generation of runaway electron seed distributions leading to sub-criticality, avalanche, or fast transfer

D.P. Brennan<sup>1</sup>, E. Hirvijoki<sup>1</sup>, C. Liu<sup>1</sup>, A.H. Boozer<sup>2</sup> and A. Bhattacharjee<sup>1</sup>

<sup>1</sup>Princeton Plasma Physics Laboratory, Princeton, NJ, USA

<sup>2</sup>Columbia University, New York, NY, USA

Corresponding Author: dylanb@princeton.edu

$$\sigma(\rho, \theta) \cdot f(\rho, \theta) = N_s$$

## Abstract:

Among the most important questions given a thermal collapse event in a burning plasma experiment such as ITER, is that of how many seed electrons are available for runaway acceleration. In this study, we use the kinetic equation for electrons and ions to investigate how different cooling scenarios lead to different seed distributions for runaway electrons. The nonlinear electron-electron collisions, as well as linear electron-ion collisions are included, with electrons and ions sourced to model impurity injection. We calculate the probability to runaway including the collisional drag of background electrons, pitch angle scattering, and synchrotron and Bremsstrahlung radiation. Projecting this probability on the distribution function determines the number of seed electrons  $N_s$ . When  $N_s$  exceeds the number of relativistic electrons needed to produce the entire equilibrium current, fast transfer to runaway current is possible. Alternatively,  $N_s$  can be small enough that the runaway process is too slow to cause any significant runaway population on the experimental timescale. Between these limits, the avalanche process determines the runaway population. We find that the conditions for fast transfer are unlikely due to the timescales for equilibration of the low and high temperature electrons given an impurity injection.

FOCUS ON Precier

Well before ITER operations begin ten years from now, we must have established a comprehensive understanding of the potential for runaway electron generation, as well as methods for their control and mitigation, as the destructive potential to the plasma facing components is severely intolerable[1]. According to some predictions, as the plasma current in ITER is raised to about 15 MA, up to 70% of this thermal electron current could be quickly converted into 10 MeV runaway electron current if the plasma temperature drops well below 1 keV for any reason, potentially endangering the integrity of the chamber walls. This makes for a unique situation in requiring an assessment based on plasma theory and computation well before critical validation experiments can be performed.

Among the most important questions given a thermal collapse event is that of how many seed electrons are available for runaway acceleration and the avalanche process. Seed electrons remain with a kinetic energy above the critical energy for runaway after a thermal quench, either natural or induced. The distribution of these seed electrons in momentum and pitch angle, along with given driving electric field and dissipative effects,

$$\frac{\partial H}{\partial t} \approx 0 \quad \text{Generally, } R \propto T, \text{ so}$$

$$\frac{dV}{dt} = 0, \quad I \uparrow \quad \text{if } T \downarrow, R \downarrow. \quad V = \frac{I}{R} R, \quad \text{so if}$$

$$V = \frac{I}{R} R \downarrow (V_e \uparrow, N_e @ V_e \downarrow). \quad \text{OR}$$

what if  $\frac{d\bar{f}}{dt} = 0$ ?

TH/P1-35

# Define Thermal Quench..

can lead to three outcomes; sub-criticality, avalanche, or fast transfer. A sub-critical distribution is one with too few electrons with high enough energy to cause any significant runaway population on the experimental timescale. An avalanche distribution is one with sufficient high energy electrons to initiate an avalanche process that would cause a significant runaway population on the experimental timescale. Last, a fast transfer distribution is one with enough high energy electrons to immediately accelerate and consume the equilibrium current faster than and without the need for collisional processes.

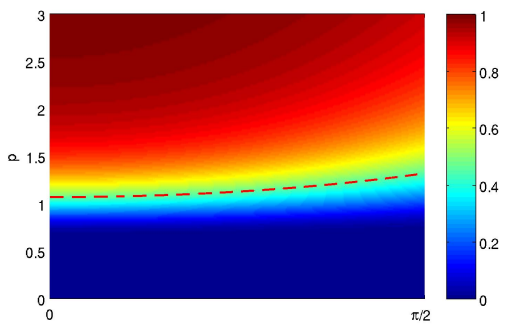


*FIG. 1: The probability of electron runaway as a function of particle momentum  $p$  and pitch angle  $\theta$ , calculated using the Adjoint method. The dashed line defines the 0.5 probability contour, above which particles can be seen as seed electrons.*

ing, and synchrotron and Bremsstrahlung radiation. A resulting probability to runaway is determined in phase space, as shown in Fig. 1. The probability for runaway has a localized transition in phase space, such that electrons with energy above this transition become highly likely to runaway. We simply multiply the probability function by the distribution function to determine the number of seed electrons  $N_s$  in the distribution

$$N_s = \int P \cdot f dv. \quad N_s : \Theta \rightarrow \mathbb{R} \quad (1)$$

When  $N_s$  exceeds the number of relativistic electrons it would take to produce the entire equilibrium current, the condition for fast transfer is met. Alternatively,  $N_s$  can be small enough that the runaway process is too slow, the condition for sub-criticality. *why do this?*

The collisional drag process dominates in impurity injection generated thermal collapses, and is generally enhanced by gas and pellet injection mitigation techniques[3]. On the other hand, the high energy population of parallel passing electrons are predominantly lost in stochastic field lines of a disruption due to MHD instability. The difference in the momentum and pitch angle dependence of these two mechanisms can cause very different outcomes in the number and distribution of remaining electrons of sufficiently high energy to run away. Several studies assume a Maxwellian background structure in the cooling process, and allow for collisional processes to calculate the response. However, to

accurately capture the remaining distribution, both the ions and electron collisions must be treated nonlinearly.

In this study, we use the kinetic equation for electrons and ions to investigate how different cooling scenarios lead to different seed distributions. We vary densities of the cold and hot populations and study how the nonlinear result varies from those assuming a Maxwellian structure. An example of this using a fully nonlinear binary collision operator is seen in Fig. 2, where a three fold increase in the cold density has nearly an order of magnitude reduction in the hot tail. Also, the effective temperature of the bulk plasma actually rises from the cold towards the equilibrium temperature in a characteristically non-Maxwellian way, and thus the assumption of a Maxwellian (ie. in test particle methods) is not completely valid in cases where the cold and hot densities do not differ by orders of magnitude.

In order to model the thermal quench and impurity deposition effects on the electron distribution function from the first principles, we include this physics in the kinetic equation. The plasma current can be constrained to be constant in time admitting a closed set of equations for self-consistent description of the thermal quench. Our model only investigates the momentum space dynamics, assuming constant profiles across the plasma and no geometric affects (ie a straight cylinder). With these approximations, the system of equations becomes relatively simple to solve, so that scans over different kinetic mechanisms can be efficiently conducted.

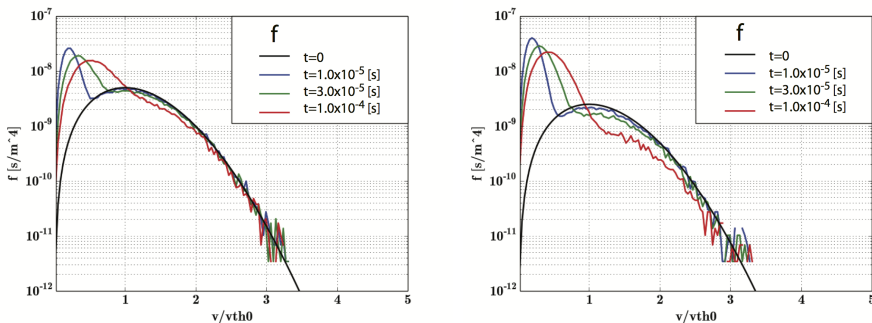


*FIG. 2: Nonlinear collisional evolution of the electron distribution. Initial plasma  $n_{e,hot} = n_{i,hot} = 10^{20} [m^{-3}]$ ,  $T_e = T_i = 20 [keV]$ , cold populations at  $T_{e,cold} = T_{i,cold} = 100 [eV]$  and  $n_{e,cold} = n_{i,cold} = n_{e,hot}$  (left) and  $n_{e,cold} = n_{i,cold} = 3n_{e,hot}$  (right). The change in the cold density has a significant effect on the hot tail, and the cooling process is clearly nonlinear.*

Our model includes a nonlinear treatment of electron-electron collisions, linear treatment of electron-ion collisions, and linear source and sink terms. Both the background and impurity ion collisions are included. The accelerating electric field is computed from the condition that the plasma current density remains constant. The concept of plasma conductivity is inherent, since the electron-electron and ion collisions are included in the model. The Spitzer response is thus automatically included.

Because the electric field in the runaway problem points to the direction parallel to the magnetic field, the cylindrical coordinate with the z-axis directed along the electric field

why?

is a natural choice. Since the distribution function is assumed to be elongated along the direction of the electric field, especially if the electric field exceeds the so-called critical field for runaway generation, we discretize our equations with Finite-Element formulation to allow use of unstructured meshes in phase space. This allows us to concentrate the mesh where it is needed, while the mesh can be very sparse in regions where it is not.

## 1 Model equations

We assume the plasma to consist of species  $a$  (electrons), which is computed from the kinetic equation, and of possibly multiple other species  $b$  (ions) which are assumed to be Maxwellian. The distribution function of species  $a$  is assumed to be affected by electric field, Coulomb collisions, and different source and sink terms, e.g., source of cold electrons from ionization of neutrals, or sink of particles mimicking the loss of plasma confinement. The kinetic model for the distribution function of species  $a$  is thus described by

$$\frac{\partial f_a}{\partial t} + \left( \frac{e_a \mathbf{E}}{m_a} \cdot \frac{\partial f_a}{\partial \mathbf{v}} \right) = C_{aa}[f_a, f_a] + C_{ab}[f_a, f_b] + L[f_a] + s, \quad (2)$$

What is this term?  
 R.F. of form  
B.F. due to  
W.P. due to  
  
 Collisional loss  
due to E field  
  
 Part of change  
due to E field  
in velocity

where the Fokker-Planck collision operator for collisions between species  $a$  and  $b$  is

$$C_{ab}[f_a, f_b] = \left( \frac{e_a^2 e_b^2 \ln \Lambda_{ab}}{m_a^2 \varepsilon_0^2} \right) \frac{\partial}{\partial \mathbf{v}} \cdot \left( \frac{m_a}{m_b} \frac{\partial \phi_b}{\partial \mathbf{v}} f_a - \frac{\partial^2 \psi_b}{\partial \mathbf{v} \partial \mathbf{v}} \cdot \frac{\partial f_a}{\partial \mathbf{v}} \right). \quad (3)$$

and the Rosenbluth potentials are

$$\phi(\mathbf{v}) = -\frac{1}{4\pi} \int f(\mathbf{v}') \frac{1}{|\mathbf{v} - \mathbf{v}'|} d\mathbf{v}', \quad \psi(\mathbf{v}) = -\frac{1}{8\pi} \int f(\mathbf{v}') |\mathbf{v} - \mathbf{v}'| d\mathbf{v}'. \quad (4)$$

The operator  $L[f_a]$  is assumed to be a general linear operator with respect to  $f_a$ . The source  $s$  is assumed to be independent of  $f_a$ . In the results presented in this paper, the source  $s$  is imposed to represent impurity injection, while the effects of the operator  $L[f_a]$  representing parallel loss in stochastic field is beyond the scope of this paper. We assume the background species  $b$  to be Maxwellian so that its distribution function is given by

$$f_b(\mathbf{v}, t) = n_b(t) \left( \frac{m_b}{2\pi T_b(t)} \right)^{3/2} \exp \left( -\frac{m_b v^2}{2T_b(t)} \right). \quad (5)$$

The kinetic equation is coupled to current conservation equation

$$\mathbf{E} \cdot \int \mathbf{v} \frac{\partial f_a}{\partial t} d\mathbf{v} = 0, \quad \text{but is this?} \quad (6)$$

which then closes our equations. The solution for  $E$  at each time is found by a Newton method. The unknowns in our implicit system are the amplitude of the electric field,  $E$ , and the distribution function  $f_a$ . Only the magnitude of the electric field is needed, since the distribution has axial symmetry along the direction of the electric field.

Because the kinetic equation is stiff, the time discretization is done by backward Euler, approximating the time derivative of the distribution function at time instance  $s$  with the expression  $\partial f^s / \partial \tau \approx (f^s - f^{s-1}) / \delta\tau$ . Further, because the space must be truncated, this requires careful treatment of the Poisson equations, and boundary conditions computed from the Green's function solution.

The formulation for the electron kinetic evolution described above is entirely classical. This allows for the careful treatment of the collisional physics at non-relativistic velocities. However, the runaway calculation must be done relativistically.

We calculate the runaway probability and seed population at any time during the simulation via the adjoint method. In the established model of runaway electron dynamics, when  $E$  is larger than the critical electric field and the radiation effect is weak, electrons initially in the high energy regime can keep getting accelerated and run away. On the other hand, electrons initially in the low energy regime will get decelerated and fall back into the Maxwellian population. Thus the destinations of electrons in the long time limit depend on their initial momentum. The radiation force can give an additional stopping power, but it can only dominate the electric force in very high energy regime when  $E$  is large. The kinetic equation for relativistic electrons can be written as [4, 5, 6],

$$\frac{\partial f}{\partial \hat{t}} + \frac{1}{p^2} \frac{\partial}{\partial p} \left[ p^2 \hat{E} f \right] + \frac{\partial}{\partial \xi} \left[ \frac{1 - \xi^2}{p} \hat{E} f \right] - \frac{1}{p^2} \frac{\partial}{\partial p} \left[ (1 + p^2) f \right] - \frac{Z+1}{2p^2} \frac{1}{p^2} \frac{\partial}{\partial \xi} \left[ (1 - \xi^2) \frac{\partial f}{\partial \xi} \right] + \frac{1}{\hat{\tau}_r} \left\{ -\frac{1}{p^2} \frac{\partial}{\partial p} \left[ p^3 \gamma (1 - \xi^2) f \right] + \frac{\partial}{\partial \xi} \left[ \frac{1}{\gamma} \xi (1 - \xi^2) f \right] \right\} = 0, \quad (7)$$

*Not even solving  
try with this  
one...*

where  $p$  is the electron momentum (normalized to  $m_e c$ ),  $\xi$  is the cosine of the pitch angle,  $Z$  is the ion effective charge  $\hat{E} = E/E_c$  where  $E_c$  is the Connor-Hastie critical electric field  $E_c = n_e e^3 \ln \Lambda / (4\pi \epsilon_0^2 m_e c^2)$  and  $\ln \Lambda$  is the Coulomb logarithm,  $\hat{t} = t/\tau$  where  $\tau$  is the relativistic electron collision time  $\tau = m_e c / (E_c e)$ ,  $\hat{\tau}_r = \tau_r / \tau$  and  $\tau_r$  is the timescale for the synchrotron radiation energy loss  $\tau_r = 6\pi \epsilon_0 m_e^3 c^3 / (e^4 B^2)$ .

In the adjoint method, we define  $P(p_0, \xi_0)$  as the runaway probability function, which means the probability for an electron that is initially at  $(p_0, \xi_0)$  to eventually run away. As shown in Ref. [2],  $P$  satisfies the homogeneous adjoint equation of Eq. (7),

$$\mathcal{E}[P] + \mathcal{C}[P] + \mathcal{S}[P] + \mathcal{R}[P] = 0, \quad (8)$$

where

$$\mathcal{E}[P] = \hat{E} \left[ \xi \frac{\partial P}{\partial p} + \frac{1 - \xi^2}{p} \frac{\partial P}{\partial \xi} \right], \quad (9)$$

$$\mathcal{C}[P] = -\frac{1 + p^2}{p^2} \frac{\partial P}{\partial p}, \quad (10)$$

$$\mathcal{S}[P] = \frac{Z+1}{2p^2} \frac{1}{p^2} \frac{\partial}{\partial \xi} \left[ (1 - \xi^2) \frac{\partial P}{\partial \xi} \right] \quad (11)$$

$$\mathcal{R}[P] = \frac{1}{\hat{\tau}_r} \left[ -\gamma p(1-\xi^2) \frac{\partial P}{\partial p} + \frac{1}{\gamma} \xi(1-\xi^2) \frac{\partial P}{\partial \xi} \right]. \quad (12)$$

The boundary conditions of  $P$  are set as  $P(p = p_{\min}, \xi) = 0$ ,  $P(p = p_{\max}, \xi) = 1$ , where  $p_{\min}$  and  $p_{\max}$  are two boundaries in momentum space that are located far from the transition region, such that the solution is insensitive to the boundary locations.

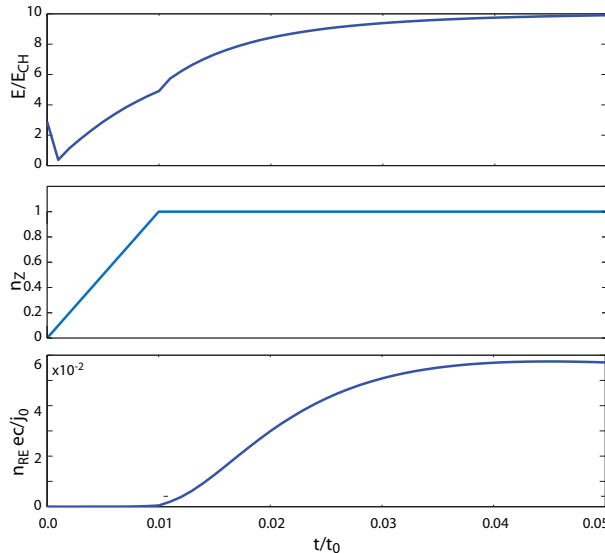


FIG. 3: The timeline of a simulation of massive impurity injection. The effective electron temperature (not shown) drops from 10keV to  $\sim 500$ eV within  $t/t_0 < 0.01$ , where  $t_0$  is the initial inverse collision frequency, though this is effectively a two temperature distribution. The electric field does not increase until much later when the cold population begins to equilibrate. The resultant seed electron population remains low.

why a + is this for )

In Fig. 3 the timeline of a simulation is shown. Prior to the timeline shown, the plasma has an initial temperature of 10keV, and a moderate constant electric field ( $E/E_{ch} < 1$ ) draws out a current which proceeds to steady state due to collisional drag on the ions. At this time a large deposition of Ar impurities occurs at low temperature (100eV), similar to Fig. 2, where a separate species of impurity ions are also introduced via a collision operator, the ion temperature is decreased, and cold electrons enter with a sourcing function. The current is then constrained in the simulation and the electric field increases rapidly to be greater than  $E_{ch}$ .

The runaway seed population is then calculated from the distribution. Using this method, the conditions for fast transfer of the runaway population are found to be difficult to achieve. The main reason for this is that when the impurities are introduced, the  $T_e$  is observed to plummet, but this is the average over all electrons, while actually there are two populations, hot and cold electrons. Over the timescale of the simulation (units are in 10keV collision times, roughly ms) the surviving hot population responds readily to support the current against the electric field, and the effective resistivity and electric field does not increase rapidly. Under conditions more extreme than expected in experiment, in the sense that the electron density increase is more rapidly, the seed runaway population

why do we need to introduce impurities?

is found to be robustly within the avalanche regime, as shown in Fig. 3. The effect of the parallel losses in this context are under investigation. In experiment, it can be very difficult to distinguish a fast transfer (100% seed) and a significant avalanche seed ( $>0.1\%$  seed). Further investigations are ongoing to determine if the conditions required for fast transfer with an accurate model for the nonlinear collisional dynamics are consistent with experimental observations.

## References

- [1] A.H. Boozer, Phys. Plasmas **22**, 032504 (2015).
- [2] Chang Liu, Dylan P. Brennan, Amitava Bhattacharjee and Allen H. Boozer, Phys. Plasmas **23**, 010702 (2016).
- [3] V.A. Izzo, E.M. Hollmann, A.N. James *et al*, Nucl. Fusion **51**, 063032 (2011).
- [4] A. Stahl, M. Landreman, G. Papp, E. Hollmann, and T. Fu?lo?p, Phys. Plasmas **20**, 093302 (2013).
- [5] P. Aleynikov and B. N. Breizman, Phys. Rev. Lett. 114, 155001 (2015).
- [6] F. Andersson, P. Helander, and L.-G. Eriksson, Phys. Plasmas 8, 5221 (2001).